Development & Validation of Low-Cost, Highly-Durable, Spinel-Based Materials for SOFC Cathode-Side Contact

Jiahong Zhu

Department of Mechanical Engineering

Tennessee Technological University (TTU)

Annual Solid Oxide Fuel Cell (SOFC) Project Review Presentation, 2020

Outline

- **Introduction and Project Objectives**

- **Performance Evaluation of the Sintered Spinel Contact Thermally Converted from Pre-alloyed Precursors**
  - **Area Specific Resistance (ASR), Chemical Compatibility, etc.**

- **Initial Study on Reaction Layer Formation Kinetics/ Mechanism**

- **Reactive Sintering of Dense $(Mn,Co)_3O_4$ Coatings**

- **Co-sintering of Spinel-Based Coating/Contact Dual-Layer Structure between Full-sized Ferritic Alloy and LSM Plates**

- **Concluding Remarks**

- **Acknowledgments**

Need of Contacting for Different SOFC Stacks

- In stacks with anode-supported cells (ASC-SOFC), the contact is required to minimize the cathode-interconnect interfacial resistance.

Cathode-Interconnect Interface in ASC SOFC Stacks

- In all-ceramic stacks, the contact is required to minimize the interfacial resistance between the current collector plate and cathode end plate.
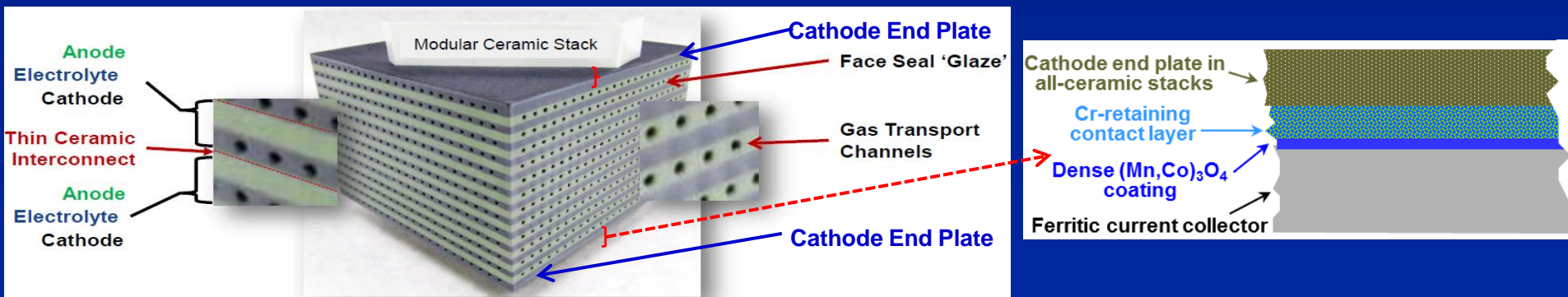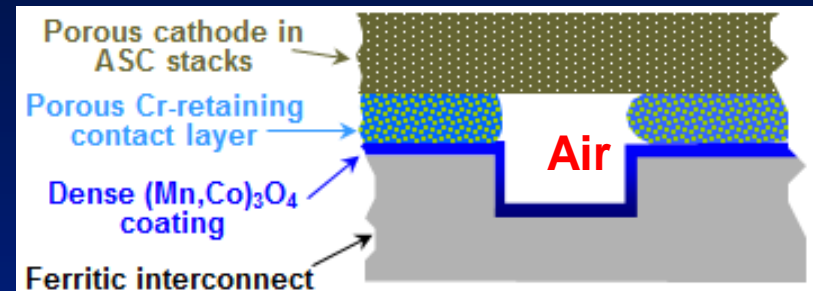

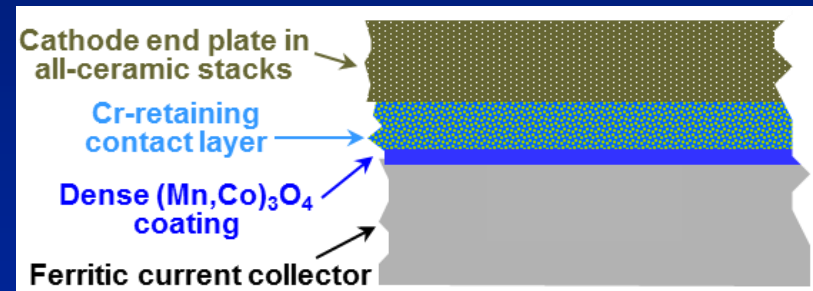*Cathode-Current Collector Interface in All-Ceramic SOFC Stacks*

Contact Material Requirements

- **Requirements for contact materials in ASC-SOFC and all-ceramic SOFC stacks are generally similar, including:**

  – **Low material/processing cost**

  – **High electrical conductivity**

  – **Match in coefficient of thermal expansion (CTE)**

  – **Adequate stability and compatibility**

  – **Appropriate sinterability**

  – **Good bonding strength with adjacent stack components**

  – **Absence of volatile species**

Cathode-Interconnect Interface in ASC-SOFC Stacks

Cathode-Current Collector Interface in All-Ceramic SOFC Stacks

- **Additionally, a reasonable porosity level in the cathode-side contact is needed in ASC stacks for maximizing the triple phase boundaries for cathodic reaction.**

Different Contact Materials

- While various materials for ferritic alloy-cathode contacting have been studied, most developments have focused on $(\underline{La},\underline{Sr})(\underline{Mn},\underline{Co},\underline{Fe},\underline{Ni},\underline{Cu})O_3$:
  - Difficulty in balancing the electrical conductivity, CTE, sinterability and chemical compatibility of the perovskites.

Material Type	Example	CTE ($\times 10^{-6}$/K) (20–800°C)	Conductivity (S·cm^{-1}, 800°C)	Main Concern
Noble Metal	Pt	10.0	Metallic	High Cost
	Pd	12.3	Metallic	High Cost
	Au	16.6	Metallic	High Cost
	Ag	22.0	Metallic	Volatility
Perovskite	$(La_{0.8}Sr_{0.2})\,CoO_{3-\delta}$	19.2 (20-1000°C)	1400	CTE Mismatch
	$(La_{0.8}Sr_{0.2})(Co_{0.5}Fe_{0.5})O_{3-\delta}$	18.3 (20-1000°C)	340	CTE Mismatch
	$(La_{0.8}Sr_{0.2})(Co_{0.5}Mn_{0.5})O_{3-\delta}$	15.0 (20-1000°C)	190	CTE Mismatch
	$(La_{0.8}Sr_{0.2})MnO_3$	11.7 (20-1000°C)	170	Sinterability
	$LaMn_{0.45}Co_{0.35}Cu_{0.2}O_3$	13.9	80	Mn/Cu Migration
Spinel	$MnCo_2O_4$	9.7-14.4	24- 89	Sinterability
	$Mn_{1.5}Co_{1.5}O_4$	10.6-11.6	55-68	Sinterability
	$NiCo_2O_4$	12.1	0.93	Sinterability
	$NiFe_2O_4$	11.8	0.3, 6.8, 17.1	Sinterability
	$Ni_{0.85}Fe_{2.15}O_4$	12.1	15.4	Sinterability

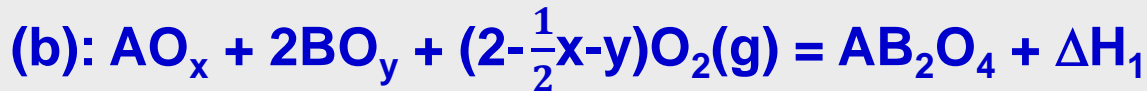# Why $(Ni,Fe)_3O_4$- and $(Mn,Co)_3O_4$-Based Spinels as Contact Material?

- **Conductive spinels based on $(Ni,Fe)_3O_4$ and $(Mn,Co)_3O_4$, which have been extensively evaluated as interconnect coating, are also promising for contact application, based on electrical conductivity, CTE, chemical compatibility, etc.**

Material Type	Example	CTE $(\times 10^{-6}/K)$ (20–800°C)	Conductivity $(S \cdot cm^{-1}, 800°C)$	Main Concern
Spinel	$MnCo_2O_4$	9.7-14.4	24- 89	Sinterability
	$Mn_{1.5}Co_{1.5}O_4$	10.6-11.6	55-68	Sinterability
	$NiCo_2O_4$	12.1	0.93	Sinterability
	$NiFe_2O_4$	11.8	0.3, 6.8, 17.1	Sinterability
	$Ni_{0.85}Fe_{2.15}O_4$	12.1	15.4	Sinterability

- **Unfortunately, the sinterability of spinels is very poor (typically ≥1000°C), if metal oxides are used as the starting powders.**

- **Employment of metallic powders (instead of oxide powders) as the starting precursor will lower the sintering temperature via a reactive sintering mechanism called <u>e</u>nvironmentally-<u>a</u>ssisted <u>r</u>eactive <u>s</u>intering (EARS).**

Utilization of EARS for Reduced-Temperature Sintering of Spinel-Based Contact

- **In EARS, with the participation of oxygen from air, the metallic powder precursor will be oxidized and reacted to form a well-sintered spinel at a reduced temperature (e.g., 900°C):**

$$\text{(b): } AO_x + 2BO_y + (2-\tfrac{1}{2}x-y)O_2(g) = AB_2O_4 + \Delta H_1$$

$$\text{(c): } A + 2BO_y + (2-y)O_2(g) = AB_2O_4 + \Delta H_2$$

$$\text{(d) \& (e): } A + 2B + 2O_2(g) = AB_2O_4 + \Delta H_3$$

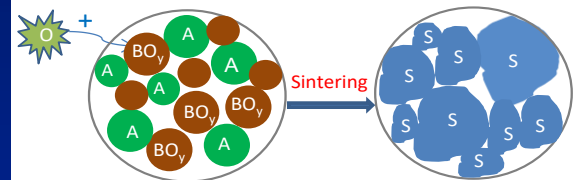$$\Delta H_3 > \Delta H_2 \gg \Delta H_1$$

- **Enhanced sintering via EARS is likely due to:**
  – **Heat released during the reaction;**
  – **Volume expansion upon conversion of metal to metal oxide;**
  – **Formation of highly-active surface nano-oxides;**
  – **Shorter diffusion distance when a pre-alloyed powder is employed.**
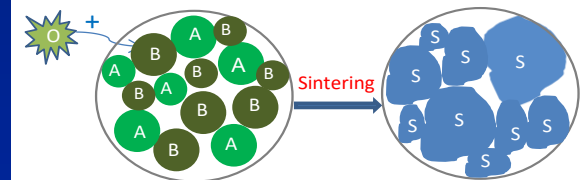
Zhu et al., IJHE, 2018
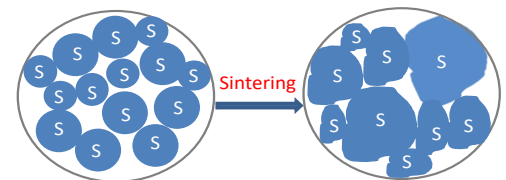
(a) with a spinel (S) powder

(b) with a mixture of metal oxides

(c) with metal and oxide powders

(d) With two metal powders

(e) With a pre-alloyed powder

Project Objectives

- **Optimization of the multi-component alloy precursor composition as contact material.** The alloy compositions will be optimized via composition screening in the $(Ni,Fe,Co,X)_3O_4$ and $(Mn,Co,X)_3O_4$ system, alloy design using physical metallurgy principles, and cost considerations. The desired alloy powders will be manufactured & characterized in detail.

- **Demonstration/validation of the contact layer performance in relevant SOFC stack environments.** Long-term ASR behavior and in-stack performance of the contact layer in relevant stack operating environments, its microstructure, chemical compatibility & Cr-retaining capability will be evaluated.

- **Further cost reduction and commercialization assessment.** Approaches to further reducing the stack cost will be explored, such as co-sintering of the interconnect coating and contact layer. Cost analysis and scale-up assessment will be conducted for potential commercialization.
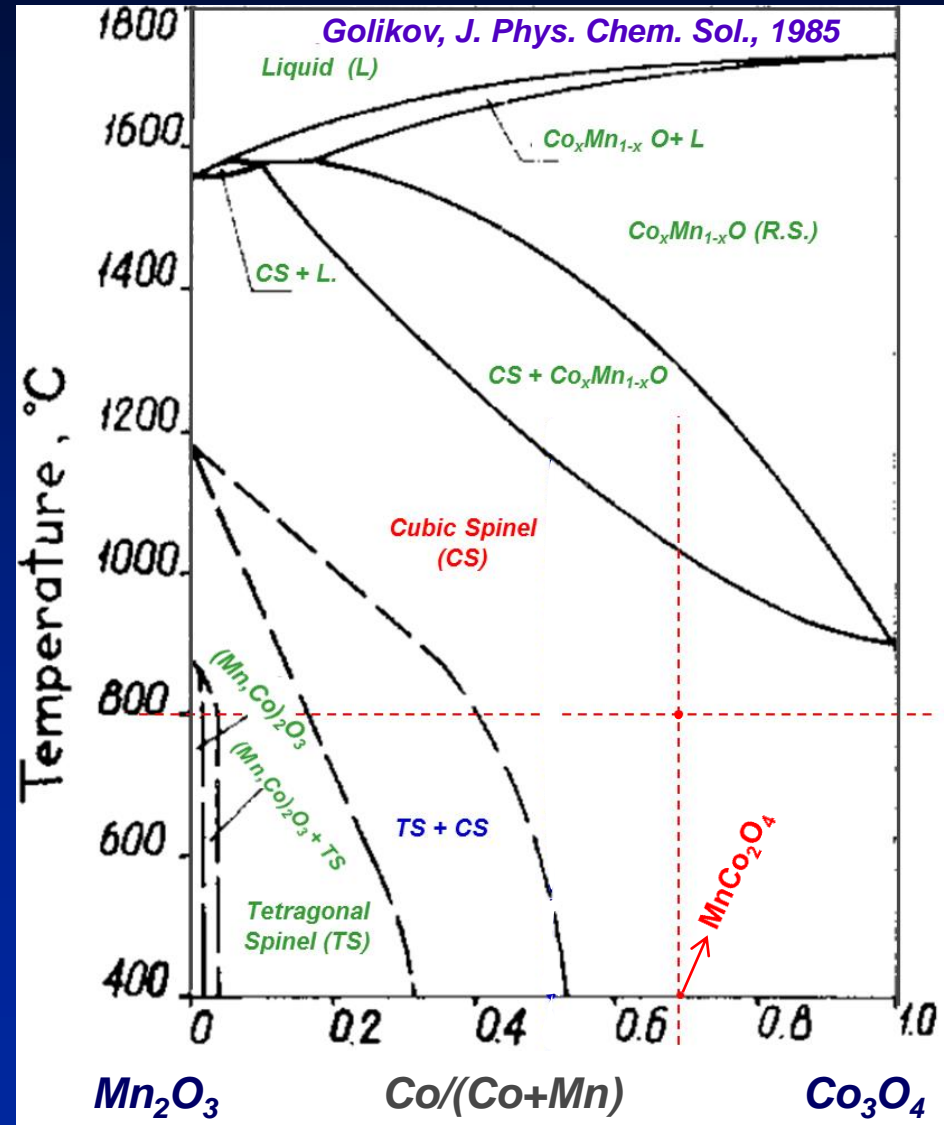
Compositional Design for Co-Mn Based Alloy Precursor

Huang, CALPHAD, 1989
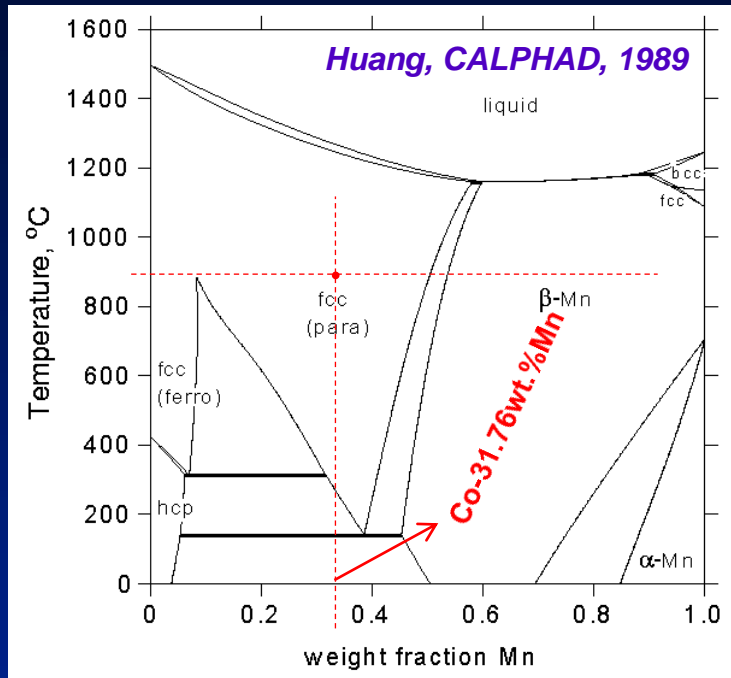
Phase Diagram of the Co-Mn System

- Co-31.76 wt.%Mn was selected as the baseline composition, which after thermal conversion would lead to the MnCo$_2$O$_4$ spinel formation:

  ✓ The Co-31.76 wt.%Mn alloy has the single-phase fcc structure at 900°C;

  ✓ MnCo$_2$O$_4$ has a cubic structure at both 800 and 20°C

Golikov, J. Phys. Chem. Sol., 1985

Phase Diagram of the Co-Mn-O System in Air

Compositional Design for Co-Mn Based Alloy Precursor

- **Fe addition to the binary Co-Mn alloy for reducing the reaction layer growth;**

- **Ce doping for slowing down the Cr_2O_3 scale growth on the alloy and improving the scale adhesion via "reactive-element effect".**

*Talic, SSI, 2019*
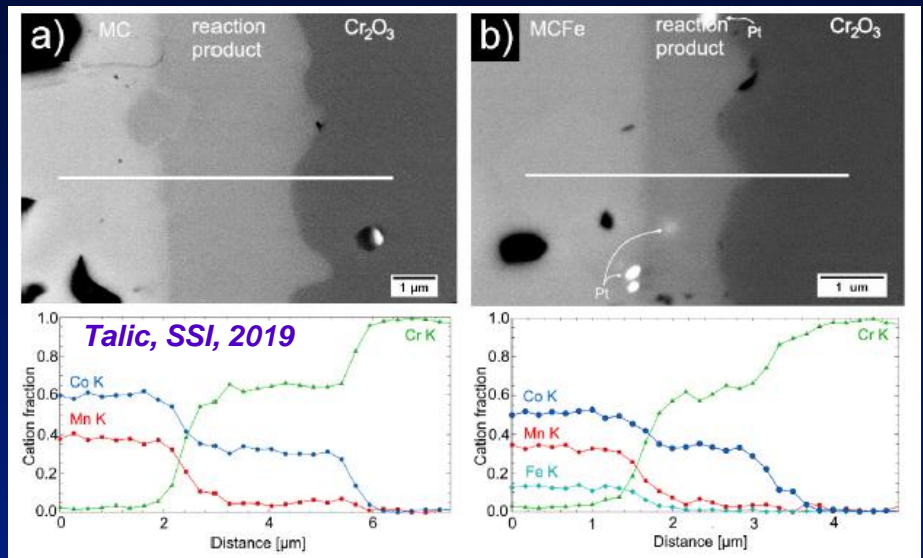
The interface of (a) $MnCo_2O_4$ (MC)/Cr_2O_3 & (b) $MnCo_{1.7}Fe_{0.3}O_4$ (MCF)/Cr_2O_3 diffusion couple after 900ºC for 300 h

Alloy Compositions & Corresponding Spinels after Thermal Conversion

(in wt.%)	Co	Mn	Fe	Ce	Spinel Composition
Alloy 1	68.21	31.79	—	—	$MnCo_2O_4$
Alloy 2	64.72	31.80	3.23	—	$MnCo_{1.9}Fe_{0.1}O_4$
Alloy 3	64.72	31.77	3.23	0.41	$MnCo_{1.895}Fe_{0.1}Ce_{0.005}O_4$

Gas Atomization of Selected Alloys

- A number of Co-Mn based compositions were selected for the powder preparation.

- The powders with the desired composition and particle size were manufactured using a semi-industrial gas atomizer.
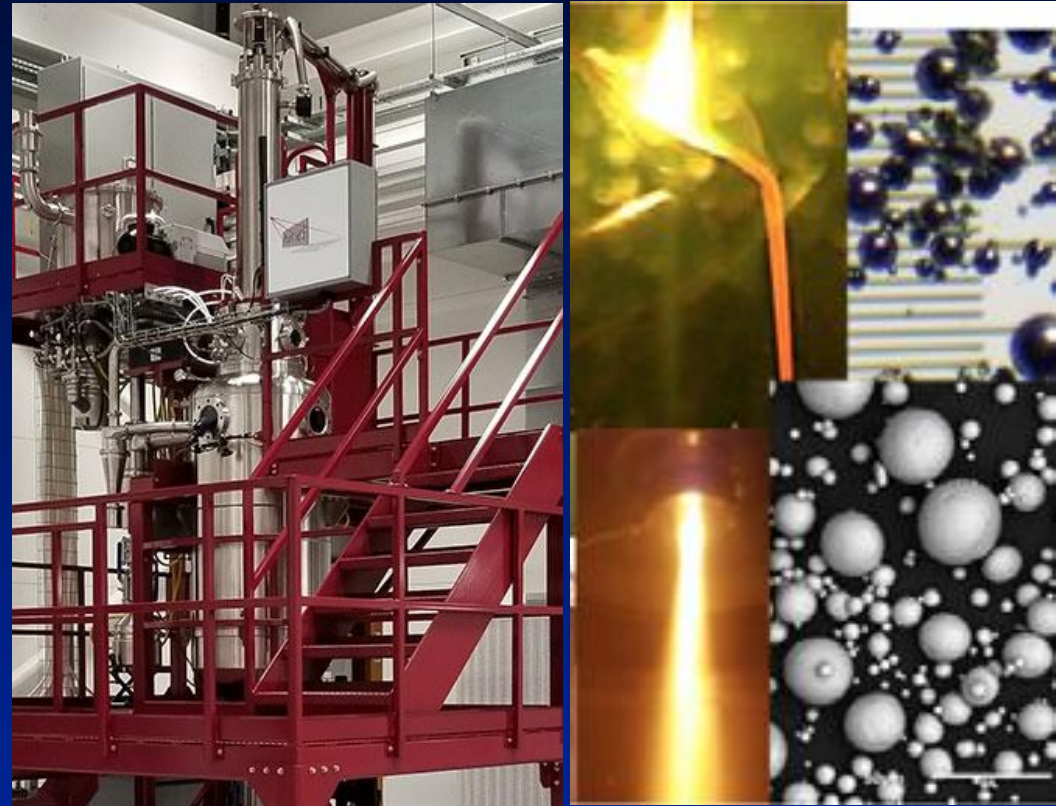

Gas Atomization System

- Chemical analysis of the collected powders was conducted at Dirats Lab – a close match with the targeted compositions was achieved.

A lab-scale gas atomizer is currently being installed at TTU under a DoD DURIP project.

Thermal Conversion of Alloy Precursors

- Three alloy powders and a $Co+MnO_2$ mixture were used as the precursor for synthesis of the desired spinel layer.

- After screen printing, the precursor layer was sintered at 900°C for 2 h in air to convert it to the spinel layer.

- A single-phase $(Mn,Co)_3O_4$ (MCO) spinel layer was formed for all the precursors.

- The alloy precursors led to narrower peaks, indicating a more homogeneous composition.
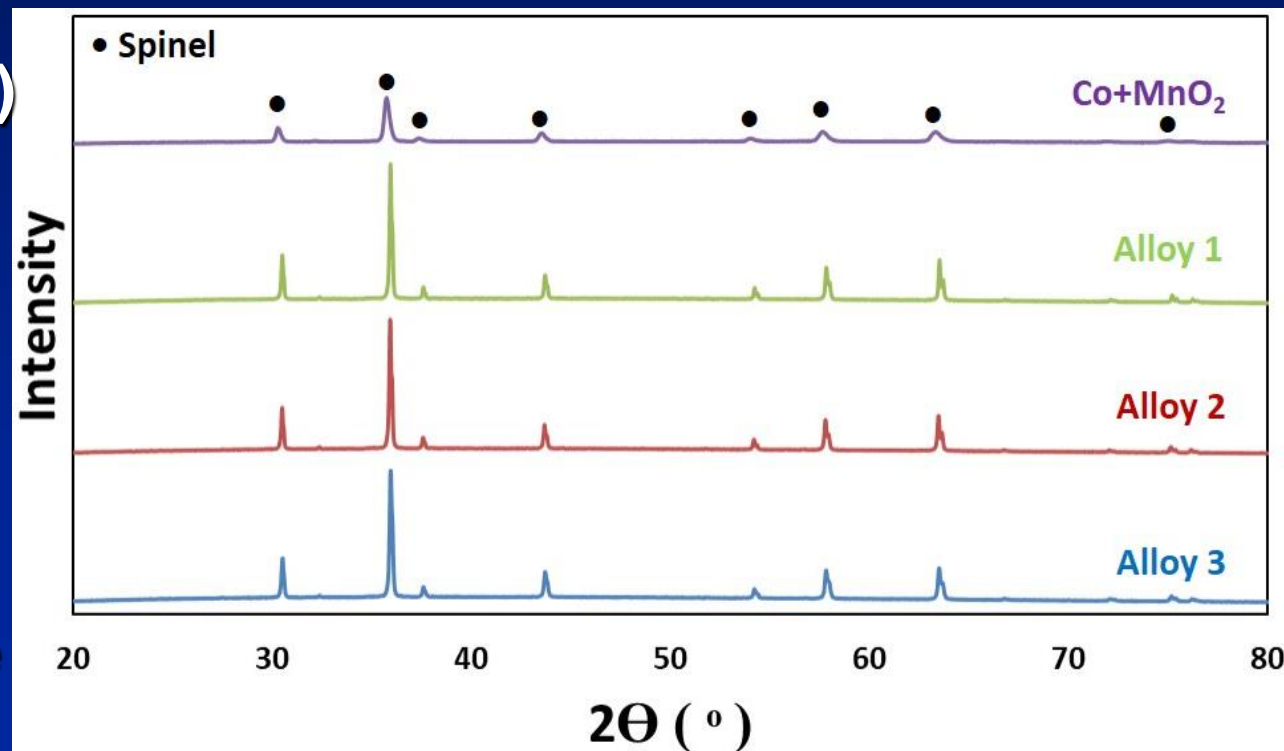
XRD Patterns of Different Precursors after Conversion

Microstructure of Converted Spinel Layer

- **The MCO layer formed with the alloy powders was more dense, compared to that with Co+MnO_2. This is a result of more volume expansion with the alloy precursor.**
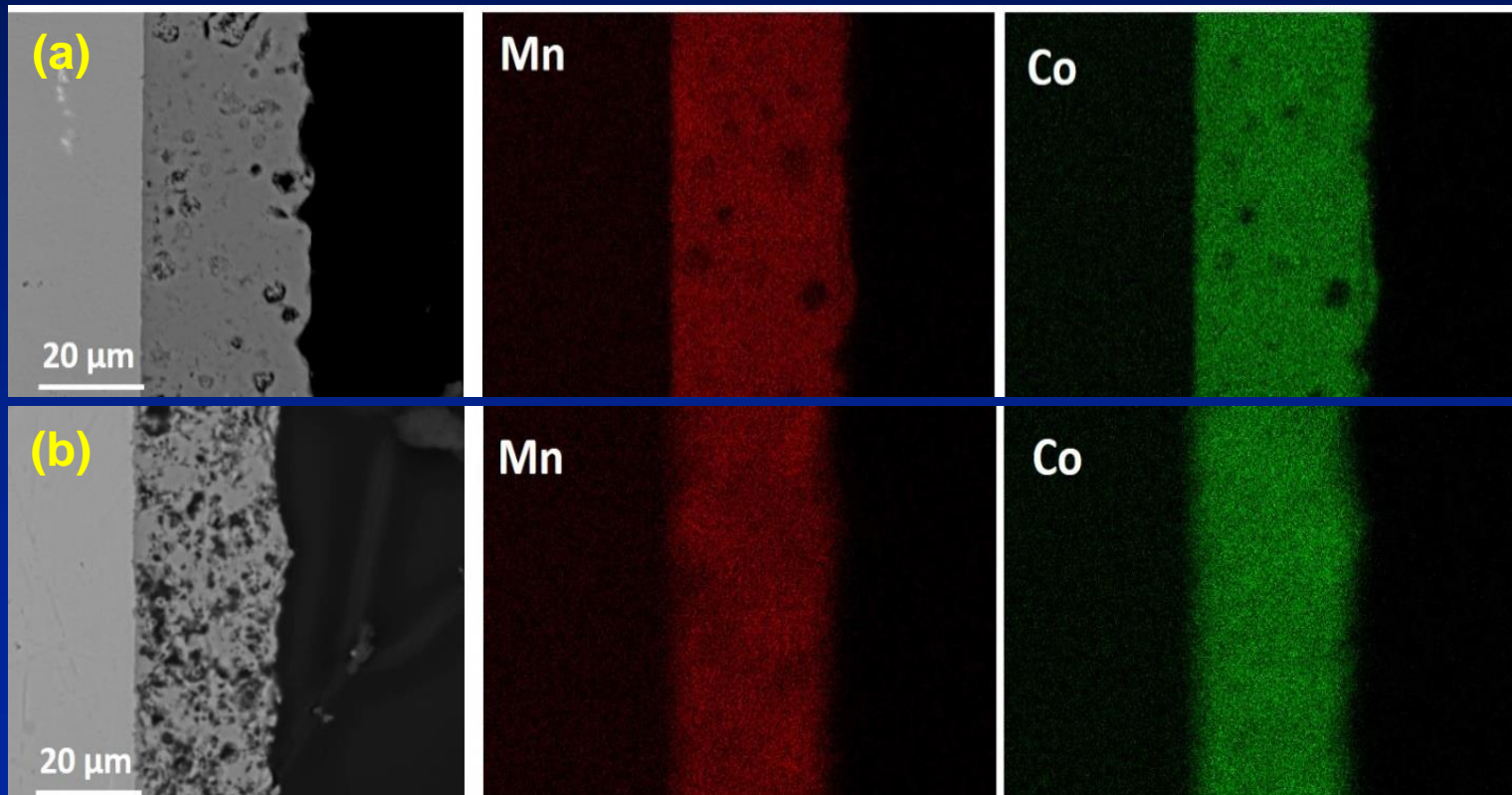
Cross-sectional View of the Spinel Layer Converted from Different Precursors: (a) Alloy 1 and (b) Co+MnO_2

Area-Specific Resistance (ASR) Measurement

- **A number of test cells were constructed, with the spinel-forming contact precursor layer sandwiched between the ferritic alloy Crofer 22 APU and the LSM cathode.**

- **The test cells were spring-loaded and heated to and held at 900°C for 2 h; after cooling down to 800°C, the cell ASR change during isothermal exposure at 800°C in air was monitored using a special 6-cell test rig.**
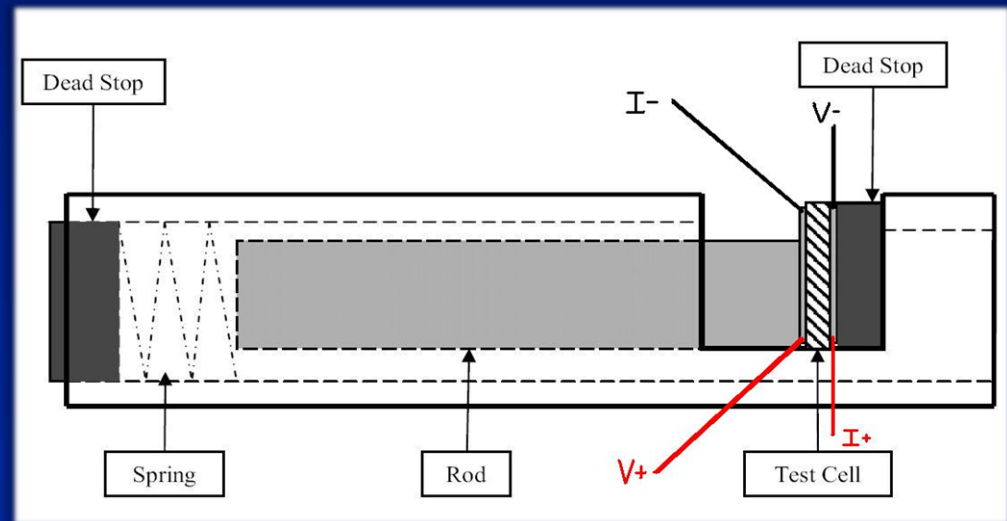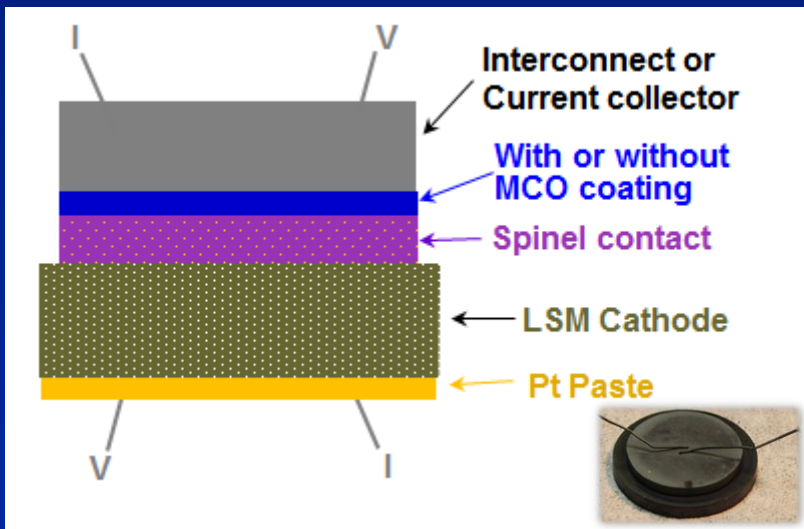

Schematic of the ASR Test Cell and Test Configuration

Cell ASR with Different Metallic Contact Precursors

- **The ASR for Crofer/contact /LSM cells with the alloy precursors was much lower than that with the Co+MnO$_2$ precursor over the duration of the test.**

- **The higher cell ASR with the Co+MnO$_2$ precursor is partially due to the higher porosities in the contact layer.**

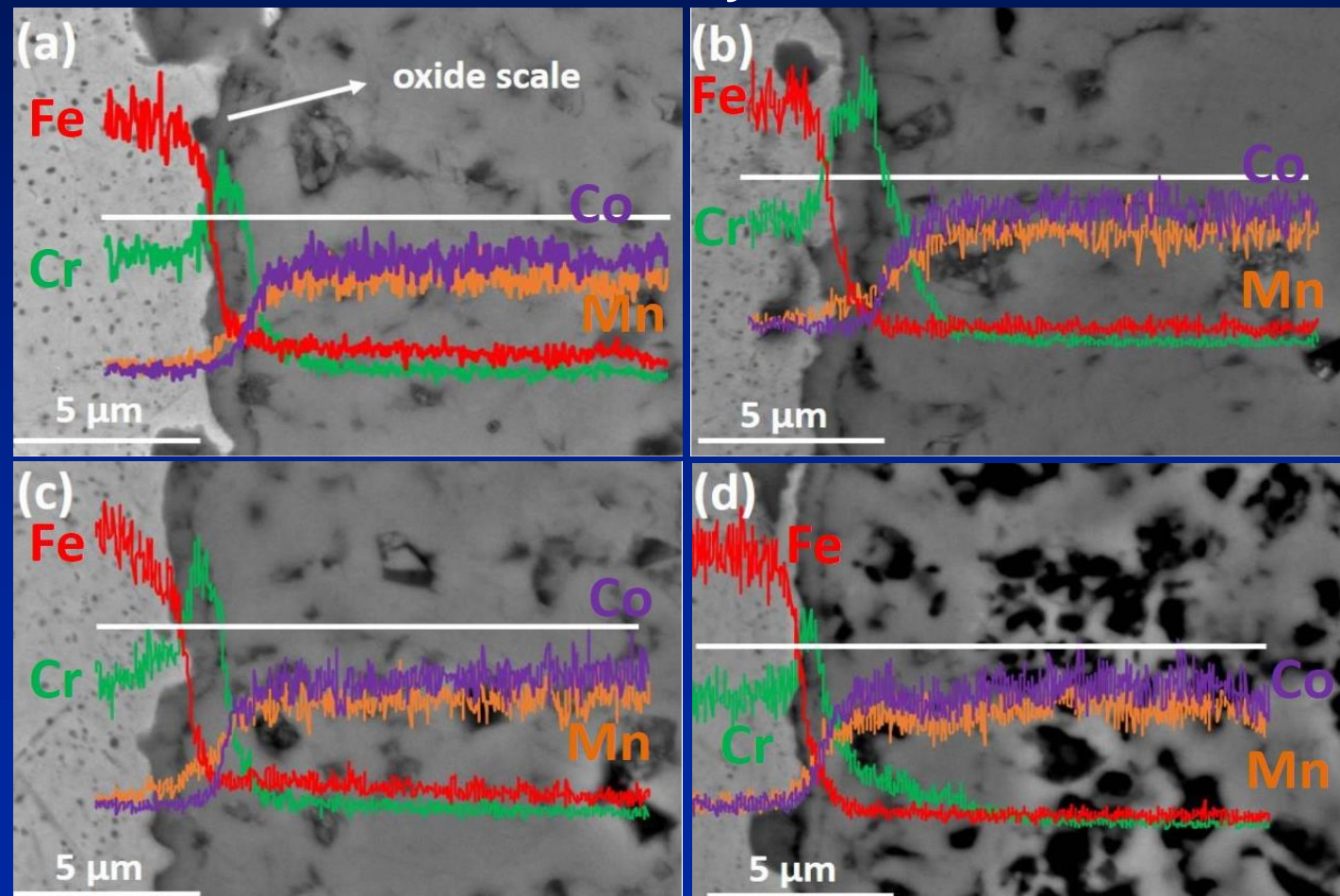**(a) Alloy 1**   **(b) Co+MnO$_2$**
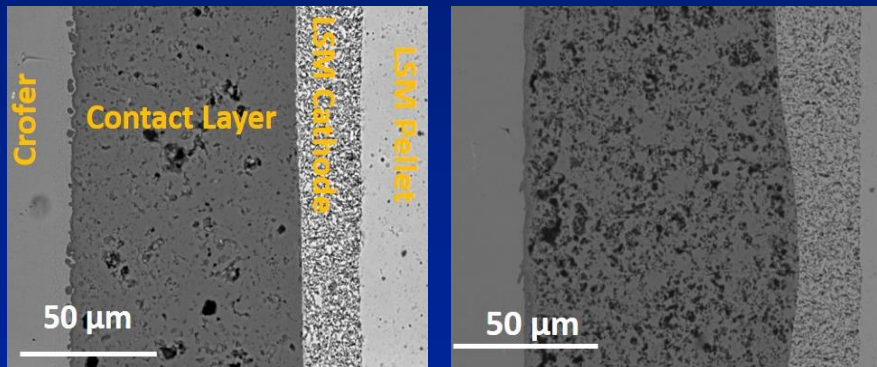
Cross Sections of Crofer/Contact/LSM cells with Different Contact Precursors
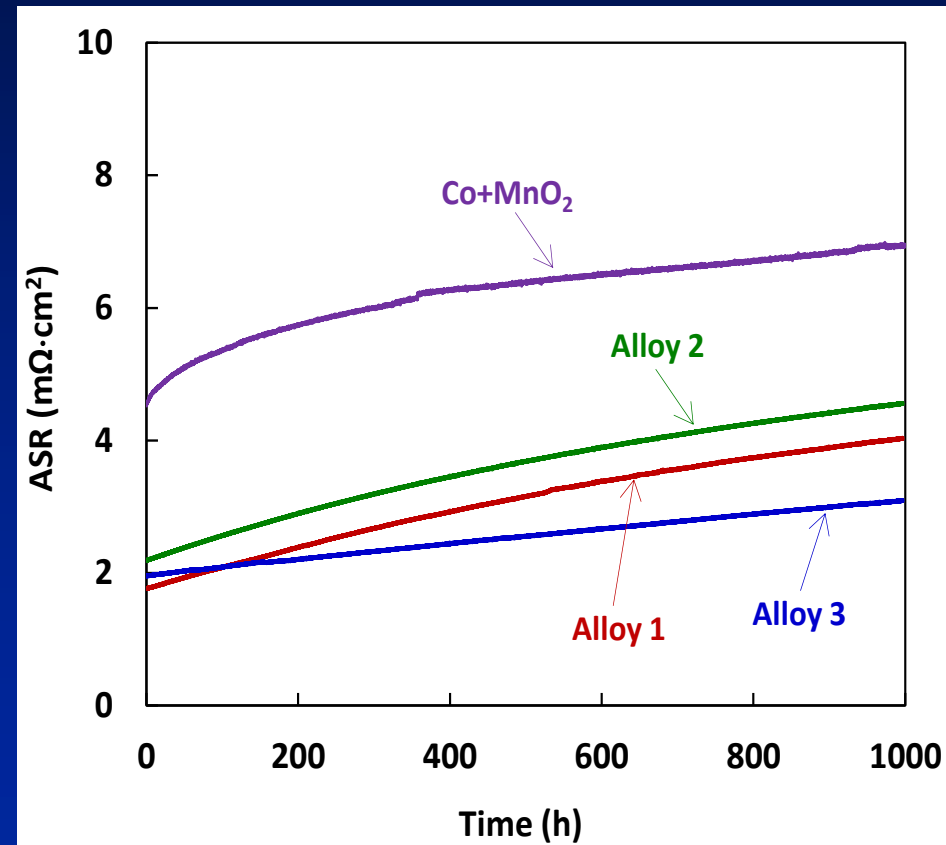
Cell ASR vs. Time at 800°C in Air

Crofer-Contact Interface: Formation of Cr_2O_3 Scale and $(Mn,Co,Cr)_3O_4$ Reaction Layer

- A Cr_2O_3 scale on Crofer 22 APU surface and a reaction layer (RL) between the Cr_2O_3 scale and the MCO contact were formed after testing.
- Alloy contact precursor composition had a significant effect on the thicknesses of these two layers.

Cross-sectional views of the ASR-tested cells with different contact precursors: (a) Alloy #1; (b) Alloy #2; (c) Alloy #3; and (d) Co+MnO$_2$. Images were taken near the Crofer-contact interface with the superimposed EDS line scans.

Summary of ASR and Cr_2O_3/Reaction Layer Thickness

– While Fe addition into the Co-Mn alloy powder had no beneficial effect on the cell electrical performance, Ce doping (in Alloy #3) led to the lowest cell ASR and ASR degradation rate as a result of slower Cr_2O_3 scale/RL growth and better scale adhesion.

Initial ASR (R_i), Final ASR after 1000-h Testing (R_f), ASR Degradation Rate during Initial 50 h (DR_o), ASR Degradation rate during Final 50 h (DR_f), and Thicknesses of the Cr_2O_3 Scale and RL after ASR Testing

	Alloy 1	Alloy 2	Alloy 3	Co+MnO$_2$
R_o (m$\Omega\cdot$cm^2)	1.8	2.2	2.0	4.6
R_f (m$\Omega\cdot$cm^2)	4.0	4.6	3.1	7.0
DR_o ($\mu\Omega\cdot$cm^2/h)	3.3	3.5	1.5	11.1
DR_f ($\mu\Omega\cdot$cm^2/h)	1.4	1.3	1.0	1.4
Cr_2O_3 scale (μm)	1.0	1.0	0.9	0.6
RL (μm)	1.4	2.2	1.4	4.5

Effectiveness of the Contact Layer in Mitigating Cr Migration
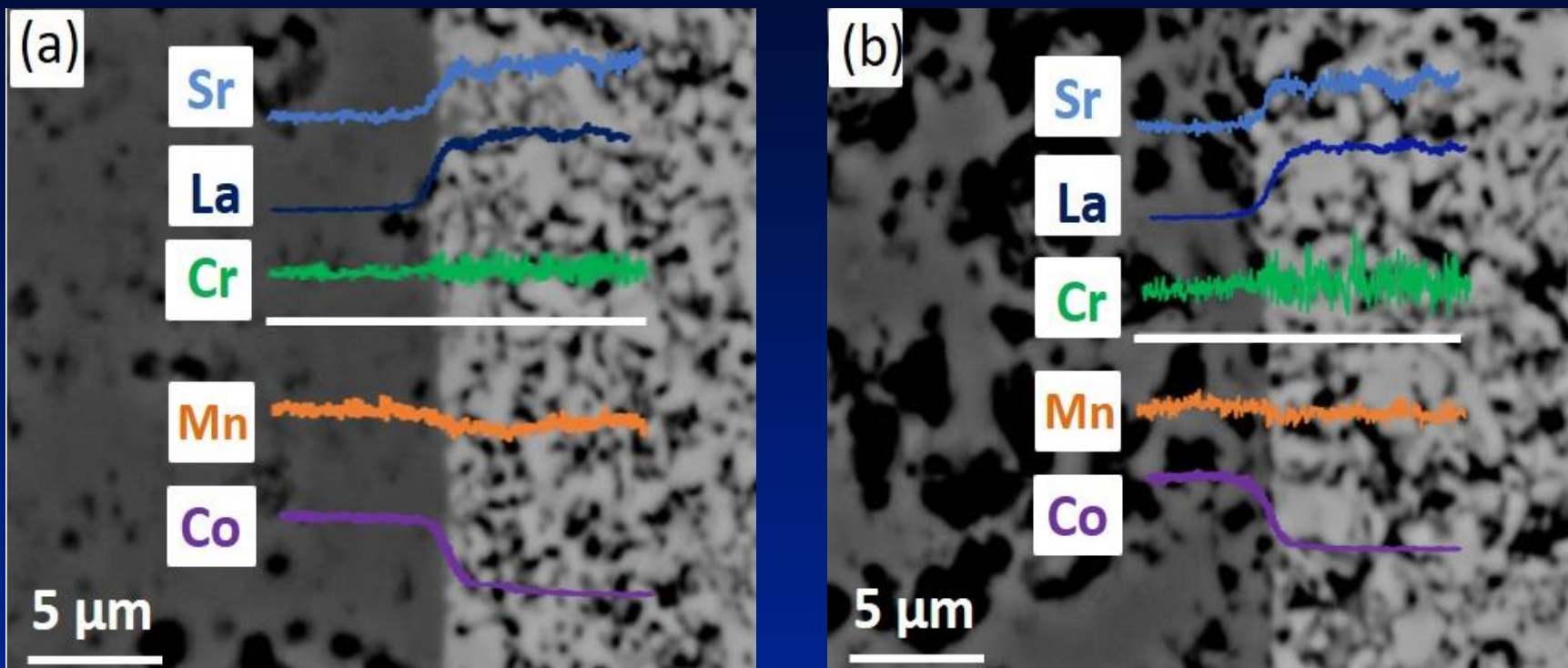
Cross-sectional View of Tested Cells near the LSM-Contact Interface with Different Contact Precursors: (a) Alloy 1 and (b) Co+MnO$_2$

– Minimal interdiffusion was observed between the contact layer and cathode for all tested cells.

– No Cr was detected in the LSM cathode for the cells with the alloy contact precursors , while for the cell with the Co+MnO$_2$ precursor the Cr level in the porous LSM cathode fluctuated noticeably.

# Preliminary Study on Reaction Layer Formation Kinetics/Mechanism

– **Since a RL was formed between the MCO layer and the Cr_2O_3 scale, it is critical to study the effect of the MCO stoichiometry and additional doping on the LR formation kinetics/mechanism:**

- **Contacting faces of MCO/Cr_2O_3 pellets were ground to 800-grit;**
- **Pt particles were applied to contacting face of MCO pellet to mark the original interface;**
- **The couple was loaded into a vertical furnace and then diffusion annealed at 900°C for different times,**
- **The annealed couples were cross-sectioned and examined with SEM/EDS.**

MCO RL Cr_2O_3

Pt mark

20 μm
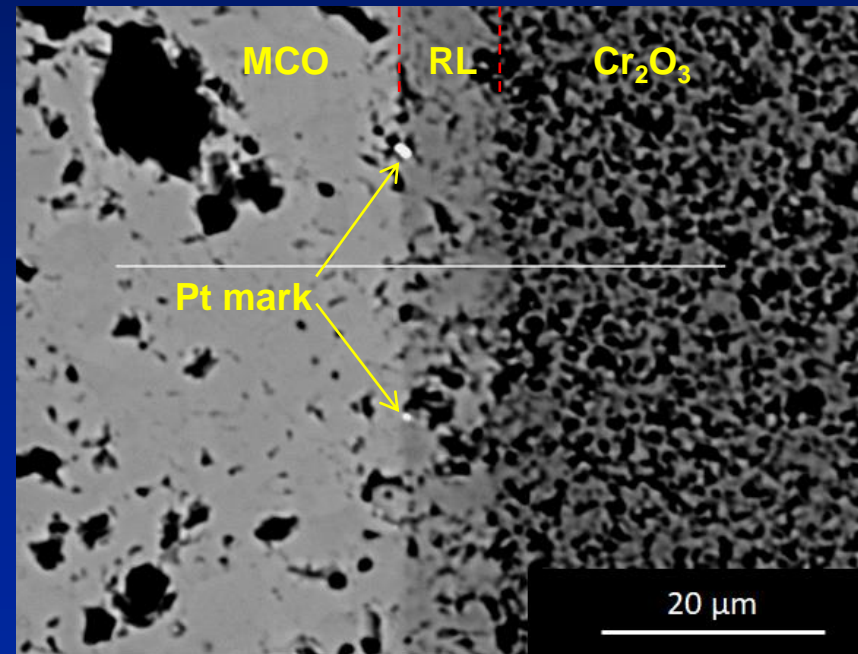
$Mn_{1.5}Co_{1.5}O_4/Cr_2O_3$ Couple after Annealing at 900°C for 300 h

Preliminary Study on Reaction Layer Formation Kinetics/Mechanism

– **A minimum in RL thickness was observed when x = 1.2 in $Mn_xCo_{3-x}O_4$.**

– **Pt marks were always observed near the MCO/RL interface, indicating the RL formation was via Co/Mn diffusion into Cr_2O_3.**

– **The RL growth kinetics is being determined.**
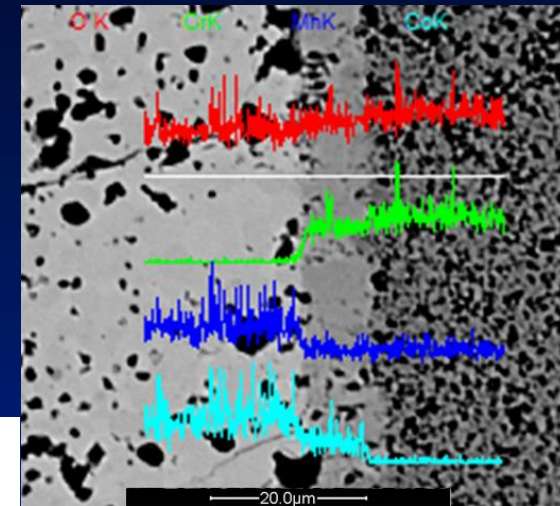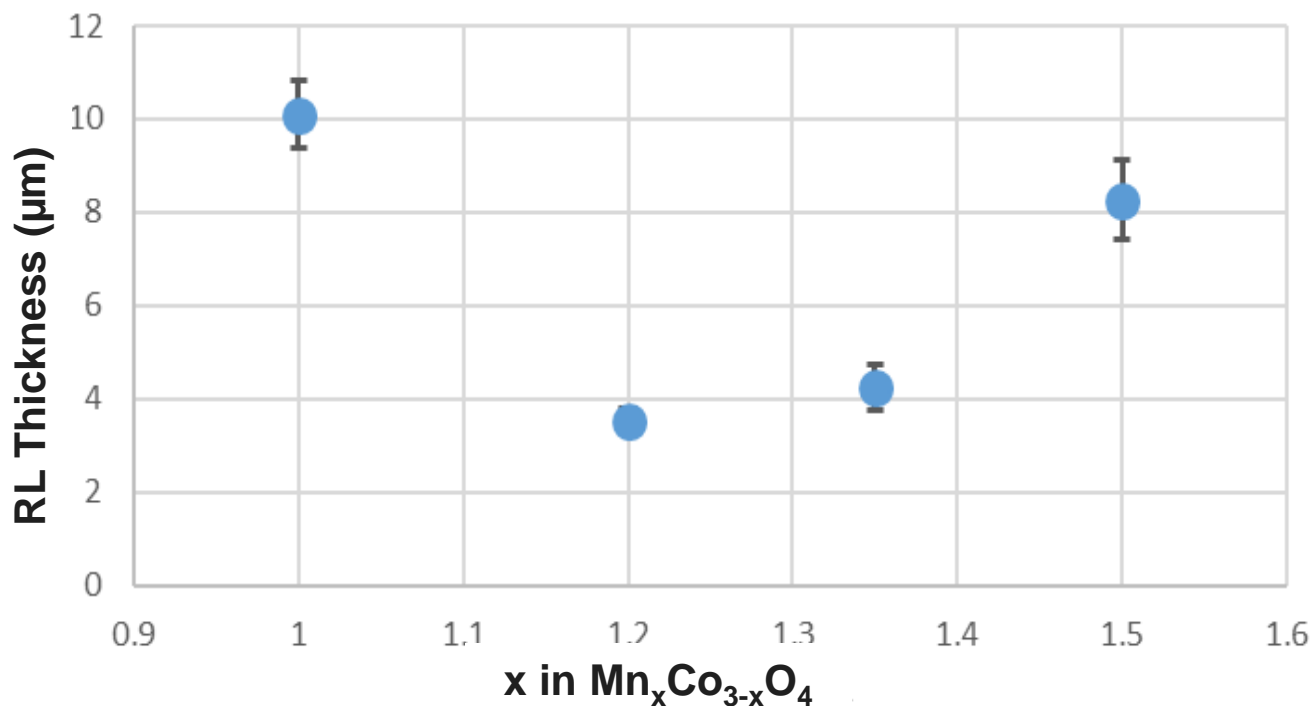
$MnCo_2O_4/Cr_2O_3$ Couple

Pt mark
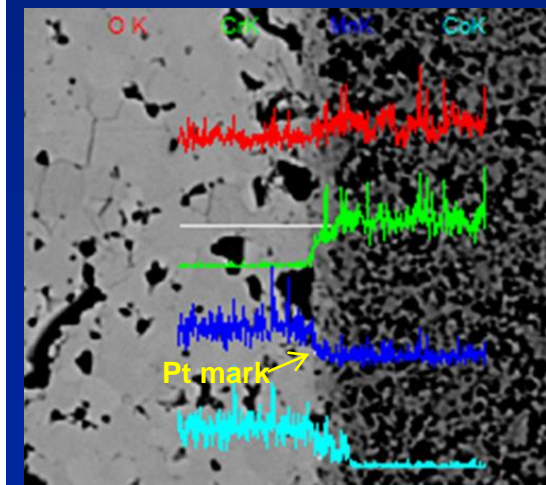
$Mn_{1.2}Co_{1.8}O_4/Cr_2O_3$ Couple

RL Thickness after 900ºCx 300-h Diffusion Anneal

EARS Processing of Dense MCO Coatings

- **Reactive sintering of a dense MCO coating via EARS has been explored and promising results were obtained:**
  - By controlling the composition/shape/size/size distribution/initial packing density of the metallic precursor powders, a dense spinel layer was obtained after thermal conversion at 900°C for 2 h in air.

- **The EARS-derived coating does not require a reduction treatment or a sintering temperature higher than 900°C, and potentially offers a better MCO coating quality.**

10 μm

Improvement in Quality of TTU's Reactive Sintered MCO Coatings on Crofer 22 APU
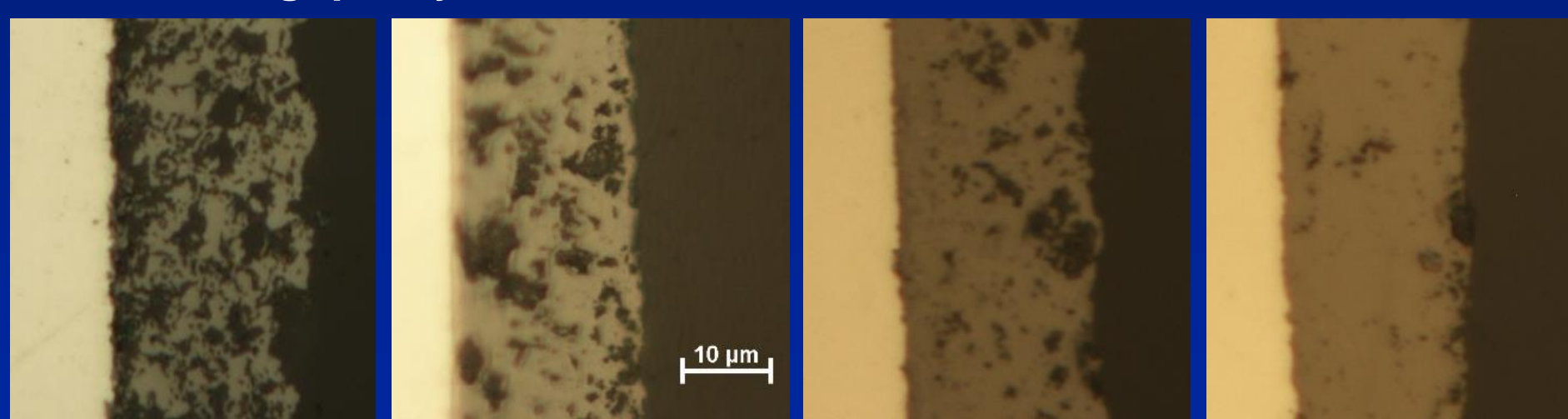
Processing MCO Coating on Full-Size ZMG 232G10 Alloy Plate

- **By optimizing the metallic spinel-forming precursor and thermal conversion conditions, a dense MCO coating was achieved, which was quite uniform in thickness and density throughout the alloy plate surfaces.**

- **The overall quality of the coating on the full-size alloy plate was comparable to that achieved on the small coupons.**

Schematic of Full-Size Plate and Cross-sectioning Locations

MCO Coating at Different Plate Locations
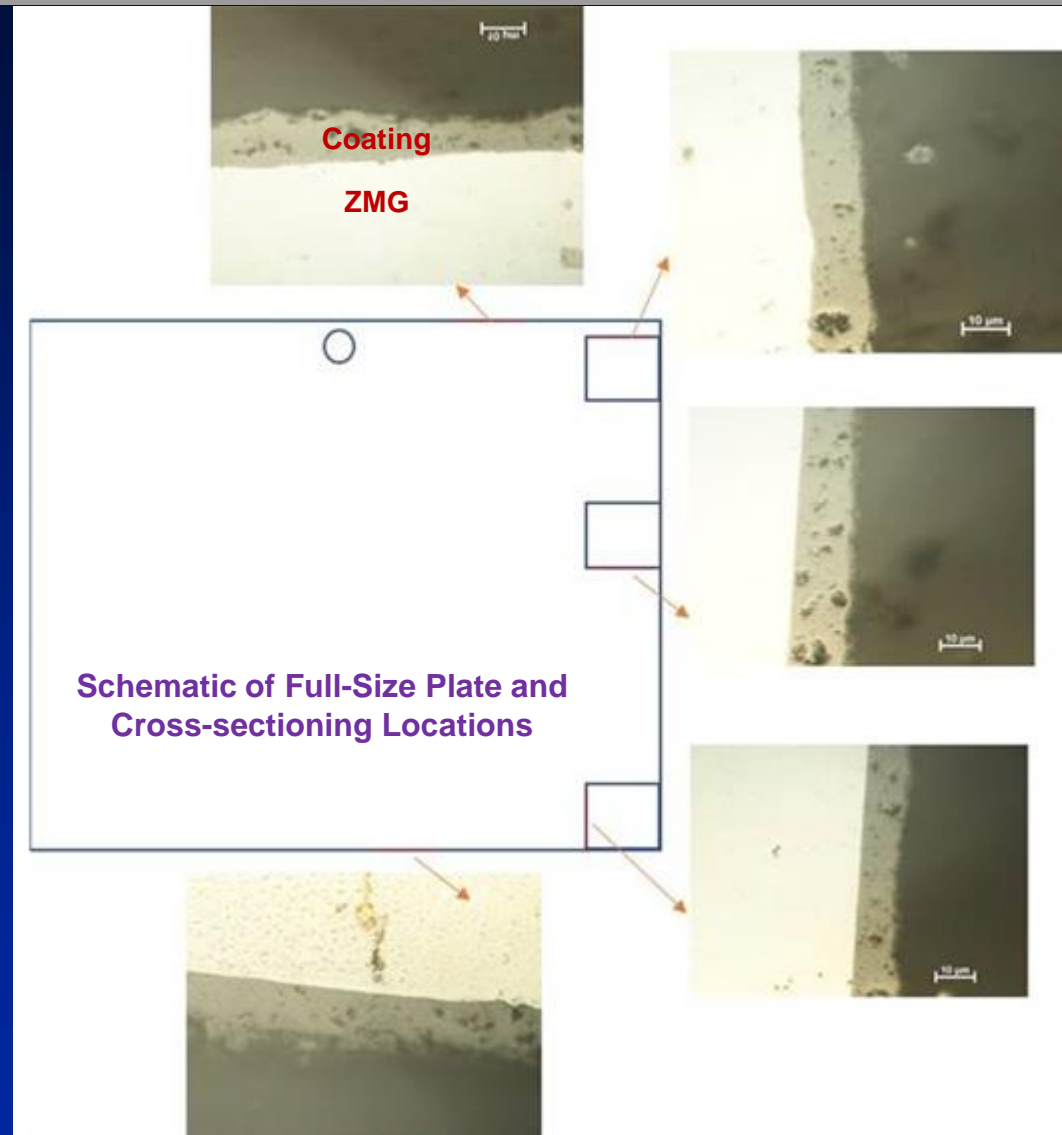
Co-sintering of Coating/Contact Dual-Layer Structure: Further Cost Reduction and Performance Improvement

- **To lower the interfacial ASR at the alloy/contact interface, improve the contact quality, and reduce the coating and contact processing cost, co-sintering of the coating and the contact layer during initial stack firing/operation is also explored, utilizing two different metallic precursors:**

  - **Two spinel-forming precursors (Type #1 – for the contact layer and Type #2 – for the dense MCO coating) will be employed;**

  - **Reactive co-sintering in air at a sintering temperature of 900°C will be utilized for simultaneous formation of the dual-layer structure.**

Cathode

Spinel-forming precursor, Type #1

Spinel-forming precursor, Type #2

Ferritic alloy

Thermal Conversion in Air @ 900°C

Cathode

Spinel contact

Dense MCO coating

Cr_2O_3 scale
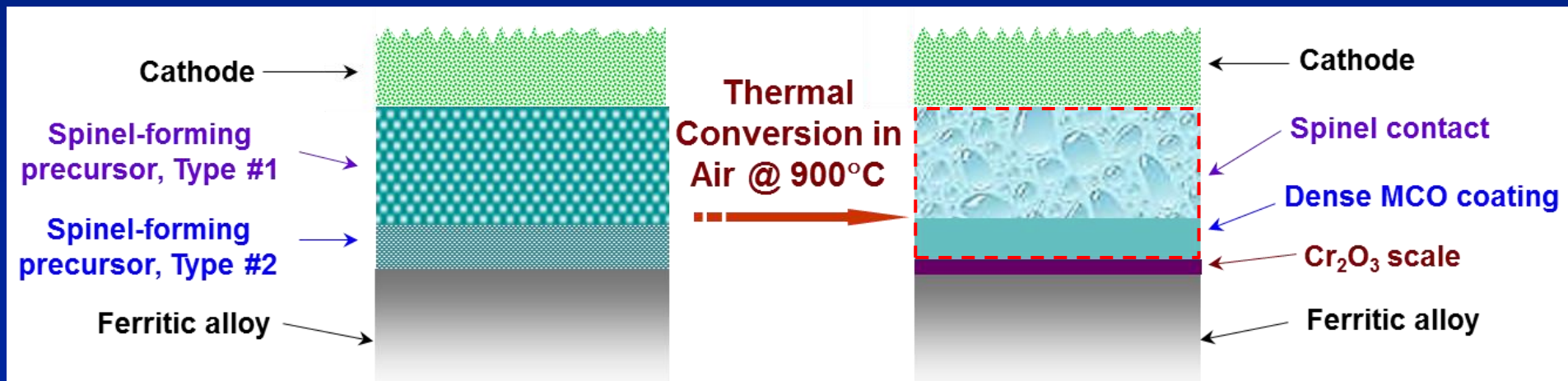
Ferritic alloy

Schematic of Co-sintering of Spinel-Based Coating/Contact Dual-Layer Structure

Co-sintering of Coating/Contact Layers between Full-Size Ferritic ZMG 232G10 Alloy and LSM Plates

- **Using full-sized alloy and LSM plates supplied by our industrial collaborator, a full-size alloy/coating/contact/LSM assembly with two metallic precursors for the coating and contact layer formation was prepared by co-sintering at 900ºC.**

  - ✓ **A dense coating and a porous contact layer between the ZMG alloy and LSM plates were achieved after co-sintering, via the utilization of two individually-optimized metallic precursors.**

  - ✓ **The thicknesses of the coating and the contact layer were 10-15 and 100-120 μm, respectively.**

  - ✓ **ASR testing of the sintered assembly is underway.**

Schematic of the Sintered Assembly

ZMG Coating Contact LSM

Co-sintered Structure at Different Locations
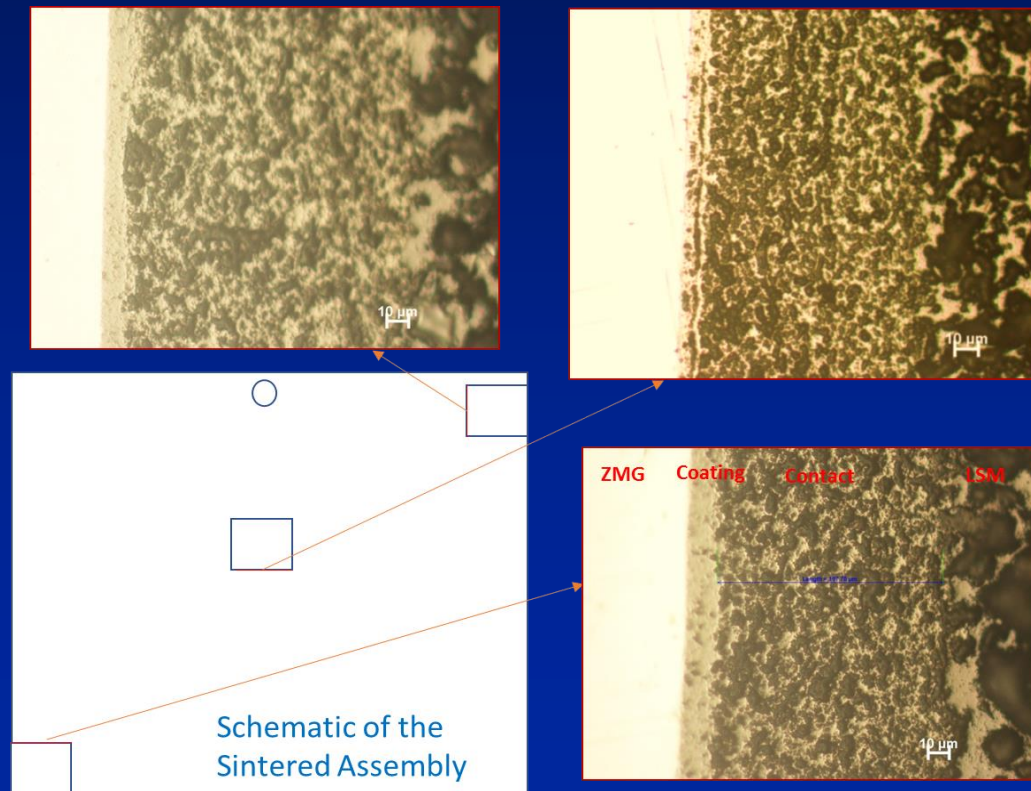
Project Milestones

Milestone Title/Description	Planned Start Date	Planned Completion Date	Actual Completion Date	Verification Method	Status
Revised PMP	10/10/2017	10/30/2017	10/23/2017	PMP file	Completed
Kickoff Meeting	10/30/2017	12/29/2017	11/29/2017	Presentation file	Completed
Compositional optimization of Precursor alloy	11/01/2017	06/30/2018	06/28/2018	Optimal Fe/Ni/Co and other alloy additions are identified.	Completed
Preparation of the alloy powder	11/15/2017	09/31/2018	09/20/2018	Atomization of one alloy powder is completed.	Completed
Demonstration of ASR stability with the new contact	01/01/2018	06/30/2019	02/20/2019	The ASR stability is demonstrated successfully for about 5,000 h.	Completed
Demonstration of stack performance stability with 1-cell stack testing	04/02/2018	09/30/2019	09/27/2019	Stack performance stability testing for $\geq$ 1,000 h is completed at industrial site.	Completed
Synthesis of dense coating on full-size current collector	10/20/2019	02/29/2020	12/25/2019	Dense coating on full-size current collector plate is achieved.	Completed
In-stack evaluation with co-sintered coating/contact structure	01/20/2020	08/20/2020		Stack power output stability testing for over 500 h is completed at Saint Gobain.	In progress
Cost analysis and feasibility assess.	06/30/2020	09/30/2020		Cost analysis and scale-up assessment are completed.	No started

Concluding Remarks

- The spinel contact-forming alloy precursor composition had a significant effect on the Cr_2O_3 scale thickness/quality, reaction layer thickness between the spinel and Cr_2O_3, and cell ASR.

- The MCO spinel stoichiometry drastically affected the thickness of the reaction layer formed between MCO and Cr_2O_3, with the $Mn_{1.2}Co_{1.8}O_4$ spinel leading to the thinnest reaction layer.

- By controlling the metallic precursor powder composition, size, size distribution, and initial powder packing density, a dense MCO coating has been synthesized on large-size ferritic alloy plate.

- Co-sintering of a dual-layer structure with a dense spinel layer as coating and a porous layer as contact can be achieved by utilizing two tailored metallic precursors between large-size alloy and LSM plates.

Acknowledgments

- **U. S. Department of Energy - National Energy Technology Laboratory, Solid Oxide Fuel Cell Prototype System Testing and Core Technology Development Program, Award No. DE-FE0031187; Project Manager: Dr. Patcharin Burke**

- **Allen Yu, Jacob Hayes, David Chesson, and Brian Bates, TTU**

- **Dr. Hossein Ghezel-Ayagh, FuelCell Energy, Inc.**

- **Dr. John Pietras and his team at Saint Gobain**